

Nosema montanae n.sp. (Microsporida: Nosematidae), a Parasite from the Grasshopper *Melanoplus packardii* (Orthoptera: Acrididae)¹

LI-YANG WANG,* D. A. STREETT,† AND J. E. HENRY‡

*Beijing Agricultural University, Department of Plant Protection, Beijing, China; and †U.S. Department of Agriculture, Agricultural Research Service, Rangeland Insect Laboratory and ‡Entomology Research Laboratory, Montana State University, Bozeman, Montana 59717

Received August 28, 1990; accepted November 15, 1990

A new species of *Nosema* was described from the grasshopper *Melanoplus packardii* (Orthoptera: Acrididae). Infections appeared to be confined to the fat body. Merogonial stages included uni-, bi-, quadri-, and multinucleate forms. Filaments or chains of meronts or early sporonts appeared to develop from the uncoiling of the multinucleate (usually octonucleate) meronts. Apansporoblastic sporonts were diplokaryotic and disporous. Binucleate sporoblasts were ovocylindrical and measured $2.7 \pm 0.5 \mu\text{m}$ by $1.6 \pm 0.3 \mu\text{m}$ in fixed, Giemsa-stained preparations. Spores were ovocylindric and measured $3.06 \pm 0.47 \mu\text{m}$ by $1.47 \pm 0.16 \mu\text{m}$ in fresh preparations and $2.8 \pm 0.5 \mu\text{m}$ by $1.4 \pm 0.2 \mu\text{m}$ in fixed, Giemsa-stained preparations. Polar tubes occurred in five to seven coils. © 1991 Academic Press, Inc.

KEY WORDS: light microscopy; ultrastructure; microsporidia; grasshopper; protozoan parasite; taxonomic description; *Nosema montanae* n.sp.

INTRODUCTION

Four species of *Nosema*, *Nosema locustae*, *Nosema acridophagus*, *Nosema cuneatum*, and *Nosema pyrgomorphae*, have been described from grasshoppers. During routine examinations of field collected grasshoppers from Montana, a microsporidium that appeared to be a new species of *Nosema* was isolated from the packard grasshopper, *Melanoplus packardii*. The characteristics that differentiated this new species from previously described species, such as spore size and shape, multinucleate meronts, and filamentous meronts, are presented here.

MATERIALS AND METHODS

Nymphs of *M. packardii* for experimental infection were obtained from eggs deposited in the laboratory by field collected adults (Henry, 1985). Each nymph was isolated without food for about 24 hr, then inoculated per os by feeding each a 7 mm diameter lettuce disk treated with 10^6

spores. After each nymph had consumed an entire lettuce disk, they were reared in groups from which individuals were randomly selected for tissue preparation at 5-day intervals beginning at 12 days after inoculation. Specimens were dissected and tissues removed for examination with phase-contrast microscopy to diagnose infection or determine tissue specificity.

For light microscopy, small fragments of fat body tissue were placed in a drop of tissue culture media (Grace or a modification thereof) on a glass slide, macerated with forceps, and air dried. Preparations were fixed in absolute methanol for 2 min, air dried, and stained in about 10% (v/v) Giemsa staining solution (Fisher) in buffer, pH 7.4 (Fisher Gram-Pac), for about 20 to 25 min at room temperature. They were transferred to buffer for 2 min, then washed in running tap water for 5 min. After drying, the slides were mounted with Crtoseal (Stephens Scientific). Measurements were performed with a filar micrometer at 1000 diameters magnification.

For transmission electron microscopy, fragments of fat body tissue were fixed for 1 hr at 4°C in 2.5% (v/v) glutaraldehyde in

¹ Mention of a proprietary product does not necessarily imply endorsement by the U.S. Department of Agriculture or Montana State University.

0.1 M sodium cacodylate (*pH* 7.4) with glycerol for an osmolality of 400 mosmol. The tissues were washed in 0.1 M sodium cacodylate buffer, postfixed for 1 hr in 1% osmium tetroxide in distilled water at 4°C, then washed twice in distilled water. The tissues were stained en bloc for 1 hr in uranyl acetate, dehydrated in acetone and embedded in Spurr's medium. Thin sections were stained with uranyl acetate followed by lead citrate and examined with a JEOL JEM-100 CX electron microscope at 100kv.

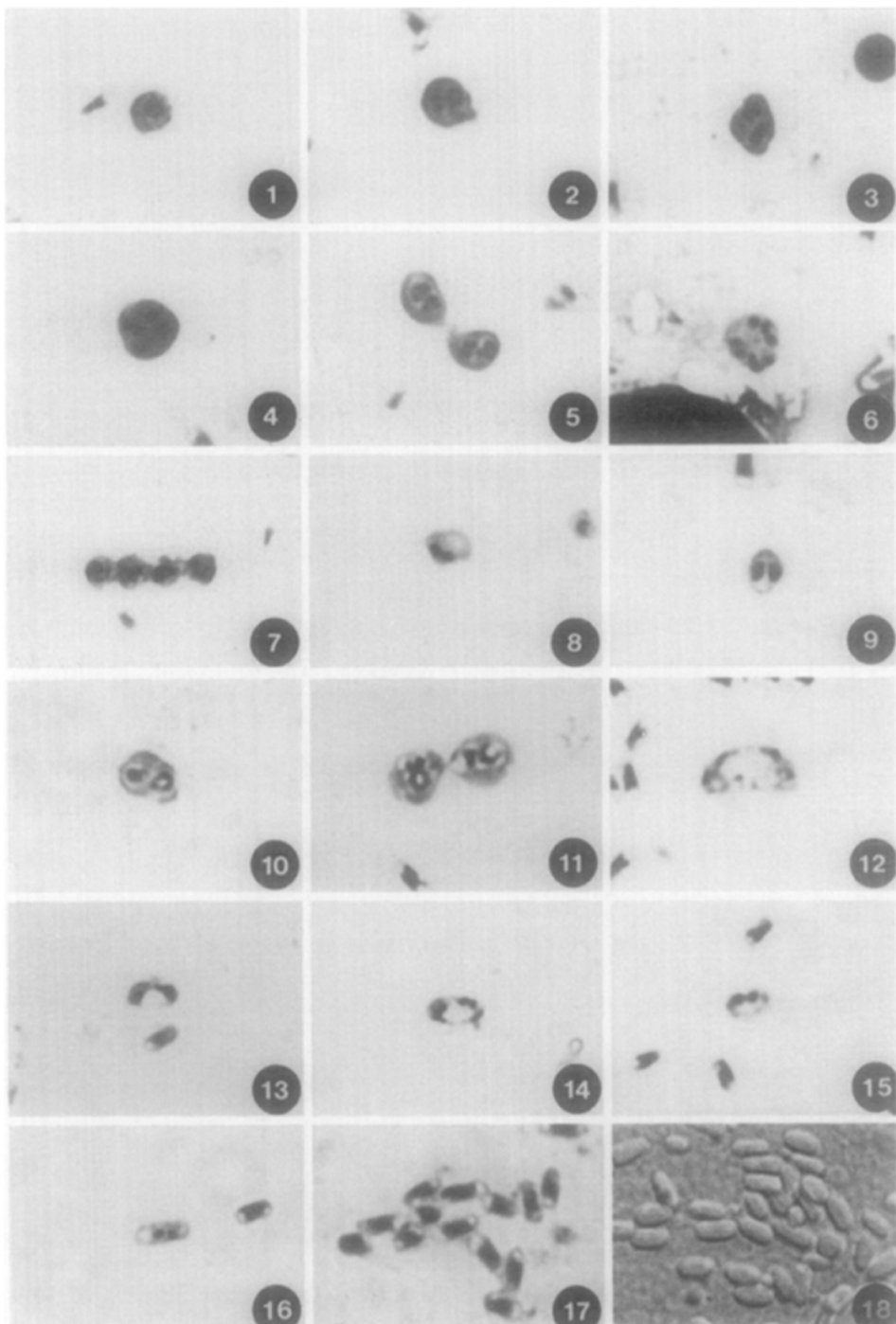
RESULTS

Light microscopy. The smallest meronts observed contained a single nucleus, were spherical and measured about 1.6 to 2.3 μm in diameter (Fig. 1). It was not evident whether or not these were diplokaryotic. Also, small spherical binucleate meronts (1.6 to 3.6 μm) were observed. In some, the nuclei were distinctly separate (Fig. 2), while in others, the nuclei appeared diplokaryotic (Fig. 3). Larger binucleate and quadrinucleate meronts (3.0 to 4.5 μm) were common (Fig. 4). Some apparently undergo cytokinesis, forming daughter meronts or possibly sporonts (Fig. 5). Larger multinucleate stages (up to 6 μm) containing six to eight nuclei were observed (Fig. 6), some of which were irregularly shaped and appeared to be changing into filamentous arrays of cells, possibly early sporonts (Fig. 7). Sporonts exhibited less basophilic cytoplasm than that of the meronts and were binucleate throughout. Smallest sporonts measured about 1.8 μm (Figs. 8,9) and the largest up to 3.6 μm (Fig. 10). Sporonts appeared to undergo cytokinesis (Fig. 11) prior to sporoblastic development. Sporoblasts (Figs. 12-15) exhibited a variety of nuclear rearrangements in the development of typical binucleate spore-shaped sporoblasts (Fig. 16). Sporoblasts measured 2.1 to 3.5 μm by 1.3 to 1.8 μm with average dimensions of 2.7 μm by 1.6 μm . Giemsa-stained spores appeared ovocylindrical (Fig. 17) and measured 2.8 \pm 0.5 μm by 1.4 \pm 0.2 μm ($N = 50$). Fresh spores were ovocylindrical (Fig. 18) and

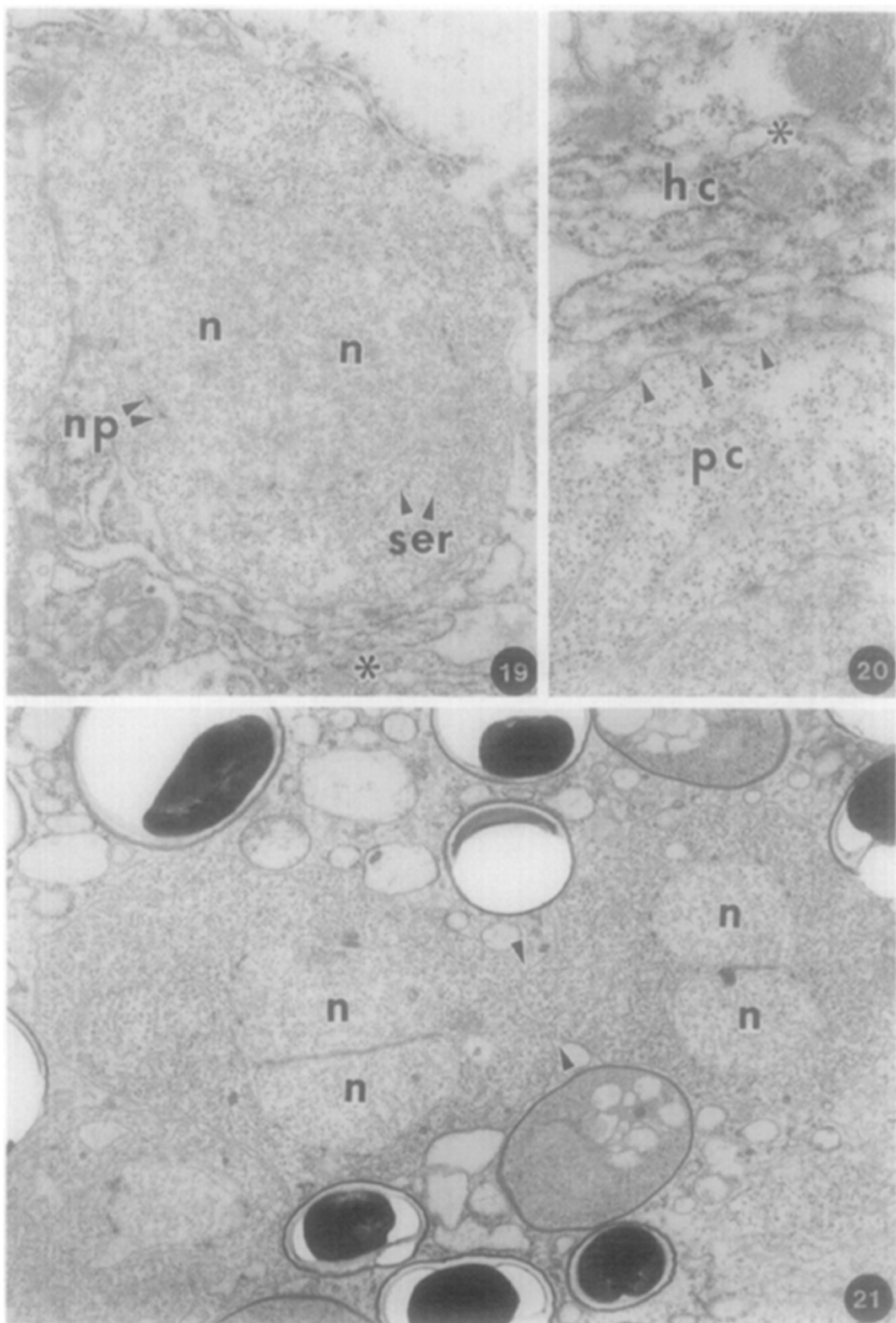
measured between 2.25 to 4.64 μm in length with a mean of $3.06 \pm 0.47 \mu\text{m}$ and 1.2 to 1.87 μm in width with a mean of $1.47 \pm 0.16 \mu\text{m}$ ($N = 50$) under Nomarski differential interference contrast. In both instances the distributions of measurements indicated some skewness toward greater lengths and widths.

Spores were present in grasshoppers 12 days after inoculation. There were no gross symptoms of infection until about 25 days after inoculation, when infected grasshoppers appeared lethargic and when mortality among inoculated grasshoppers was higher than among apparently healthy grasshoppers. Maximum spore concentrations in inoculated grasshoppers were about 5×10^9 spores per insect. Infections appeared to be confined to the fat body. No evidence of patent infection was observed in the prothoracic gland, gastric caeca, digestive tract, malpighian tubules, or pericardium. Experimental inoculation of the lesser migratory grasshopper, *Melanoplus sanguinipes*, failed to produce patent infections.

Electron microscopy. Intracellular meronts were rounded with diplokaryotic nuclei, which measured about 2 μm in diameter, and were surrounded by smooth endoplasmic reticulum (ER) with numerous ribosomes (Fig. 19). The thin meront plasmalemma was in close proximity to the host membrane, the area behind which was frequently rich with host rough ER (Fig. 20). Multinucleate meronts with two diplokaryotic nuclei were common and were usually observed undergoing cytokinesis (Fig. 21). Karyokinesis in meronts, as well as sporonts, was indicated by the occurrence of centriolar plaques which were frequently associated with 2-3 polar vesicles and kinetochore microtubules (Fig. 22). Sporonts were differentiated from meronts by the thickened plasmalemma (Fig. 23) which developed into a trilaminar membrane (Fig. 24). Electron-lucent vesicles commonly occurred in the host cytoplasm in close juxtaposition to parasites with variably thickened plasmalemmas (Fig. 25). With the development of the thickened plasmalemma,



Figs. 1-18. Light microscopy. Fig. 1. Uninucleate meront (2975 \times). Figs. 2,3. Binucleate meront (2975 \times). Fig. 4. Quadrinucleate meront (2975 \times). Fig. 5. Division of quadrinucleate meront into binucleate daughter meronts (2975 \times). Fig. 6. Octonucleate meront (1105 \times). Fig. 7. Chain of four meronts or early sporonts (1275 \times). Figs. 8,9. Binucleate sporonts (1360 \times). Fig. 10. Late sporont (2720 \times). Fig. 11. Sporogonic cytokinesis (2720 \times). Fig. 12. Early sporoblast (2720 \times). Figs. 13,14,15. Sporoblasts in various nuclear configurations (2125 \times). Fig. 16. Late binucleate sporoblast and spore (2125 \times). Fig. 17. Giemsa-stained spores (2380 \times). Fig. 18. Spores in fresh preparation under Nomarski differential interference contrast (2295 \times).



FIGS. 19–30. Transmission electron microscopy. Symbols: c, cytoplasmic vesicles; cp, centriolar plaque; en, endospore coat layer; ex, exospore coat layer; hc, host cytoplasm; mt, microtubule; n, nucleus; np, nuclear pore; pb, polar body; pc, parasite cytoplasm; pl, polaroplast; pt, polar tube; ser, smooth endoplasmic reticulum.

FIG. 19. Diplokaryotic meront with nuclear pores along nuclear membrane and a cytoplasm with smooth endoplasmic reticulum. Asterisk indicates an undefined vesicular structure that was observed in the host cytoplasm in close proximity to the parasite ($17,000\times$).

FIG. 20. Plasmalemma of a meront (see arrows) was closely surrounded by host cytoplasm with an abundance of rough endoplasmic reticulum and a undefined vesicular structure (note asterisk) ($56,100\times$).

FIG. 21. A meront undergoing cytokinesis to form two diplokaryotic daughter cells. The arrow marks the constriction between the dividing cells ($14,025\times$).

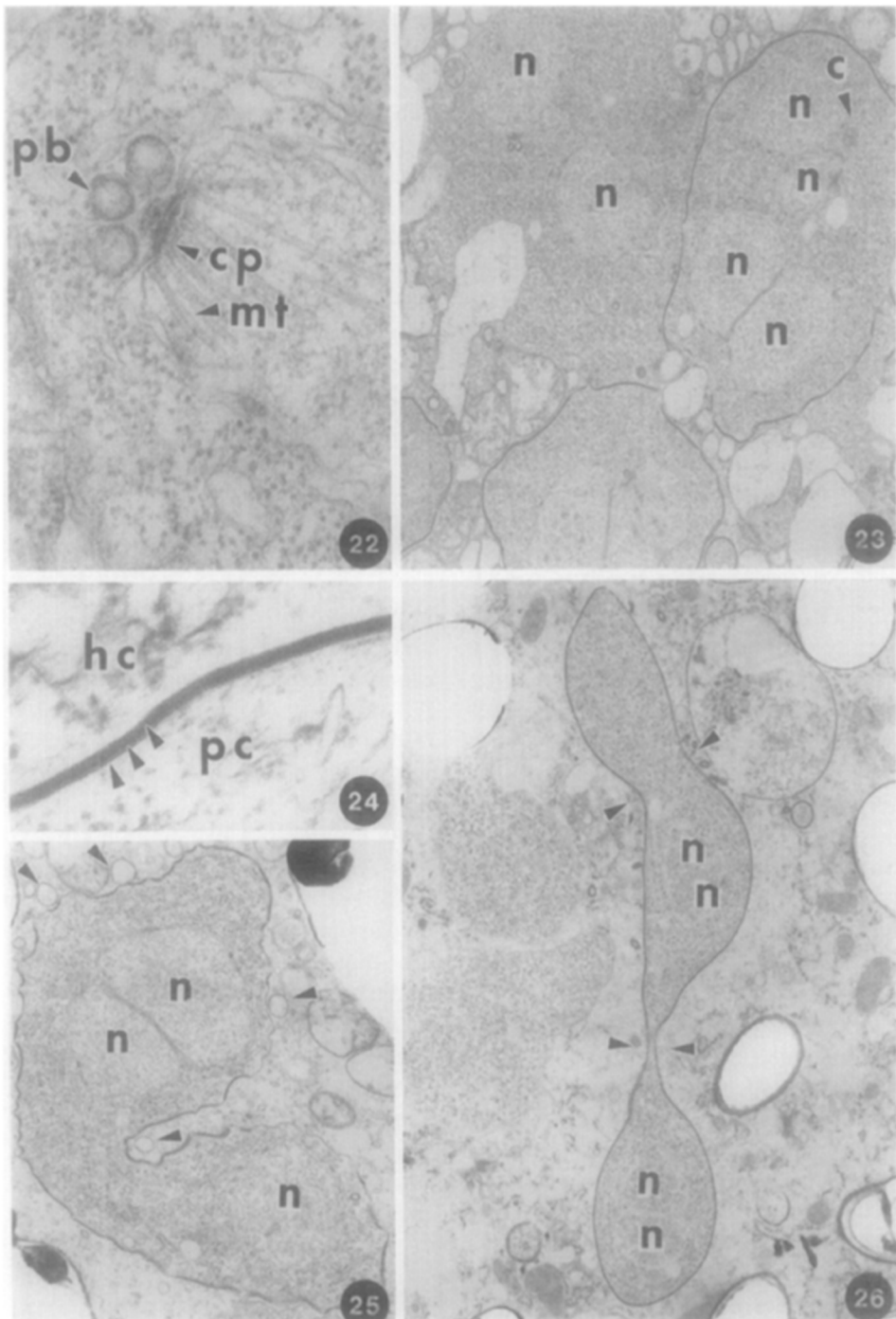


FIG. 22. A centriolar plaque in a meront with three polar bodies and radiating microtubules (56,100 \times).

FIG. 23. A binucleate meront and quadrinucleate (two diplokarya) sporont containing an undefined vesicular structure (10,200 \times).

FIG. 24. Indication of the trilaminar structure (arrows) of the exospore layer deposited around the sporont (88,400 \times).

FIG. 25. A dividing sporont showing the vesicular bodies (arrows) that may function in the deposition of the exospore layer (13,260 \times).

FIG. 26. A chain of three sporonts showing constrictions (arrows) at points of separation (8,500 \times).

there appeared to be less host rough ER near the parasite body. Elongated sporonts often appeared to be undergoing cytokinesis (Figs. 25,26). Also, sporonts were observed undergoing karyokinesis without evidence of cytokinesis, and these nuclear divisions were synchronous within a given cell. Both kinetochore microtubules, that extend from centriolar plaques to chromatin bundles, and nonkinetochore microtubules, that extend between centriolar plaques, were observed (Fig. 27). The nonkinetochore microtubules were slightly larger in diameter (25 nm) than the kinetochore microtubules (21.9 nm). Apparent golgi bodies were commonly observed in actively differentiating sporonts (Figs. 27,28). Centriolar plaques appeared to be double layers of electron dense materials (Figs. 22,27).

Typically shaped sporoblasts with polar tubes were binucleate (Fig. 29). The cytoplasm contained a rich supply of smooth ER and ribosomes. Sporoblasts and spores showed 5 to 7 coils of the polar tube. Mature spores also were binucleate (Fig. 30) and possessed a typical bilayered spore coat with the endospore layer measuring about 125 nm thick and the exospore layer about 12 nm thick.

DISCUSSION

The observations of the developmental stages of this microsporidium isolated from the grasshopper *M. packardii* establish that it is apansporoblastic, monomorphic, disporous, and predominantly diplokaryotic throughout its life cycle. Accordingly, this species is assigned to the genus *Nosema*, based on the characteristics of the type species *Nosema bombycis*. The occurrence of multinucleate meronts, usually with four diplokarya and chains of meronts and/or sporonts, has been reported for other species of *Nosema* (Kellen and Lindegren, 1969; Gray et al., 1969; Canning and Olson, 1980; Brooks et al., 1985). Although there appears to be various means by which a chain of cells can develop, our observations

indicate that it occurs directly by an uncoiling process of the multinucleate stages. As suggested by Brooks et al. (1985) the occurrence of such chains of cells is of little or no apparent taxonomic significance since they occur in various groups of microsporidia.

Electron-lucent vesicles in the host cell cytoplasm appeared near the variably thickened parasite plasmalemma. These appeared during the transition from meront to sporont and were probably involved in the thickening of the plasmalemma that signals the onset of sporogony. Vesicles or tubule-like bodies, associated with the plasmalemma of meronts during deposition of the electron-dense material that ultimately forms the exospore layer, occur quite commonly in *Nosema*. Similar structures were reported by Youseff and Hammond (1971) in *Nosema apis*, Canning and Sinden (1973) and Avery and Anthony (1984) in *Nosema algerae*, Toguebaye and Marchand (1984) in *Nosema henosepilachnae*, Brooks et al. (1985) in *Nosema epilachnae* and *Nosema varivestis*, and Streett and Henry (1987) in *N. cuneatum*.

As pointed out by Sprague (1977) the genus *Nosema* is a heterogeneous group. Also, because of the large number of species assigned to *Nosema*, it becomes virtually impossible to compare an apparently undescribed species with all others. As mentioned by Brooks et al. (1985) ordinal specificity generally is relied on to delimit species of microsporidia. In this respect the species described from *M. packardii* is quite different, based on spore size, from the other species of *Nosema* described from Acrididae, as well as other microsporidia known from Orthoptera. Similarly, multinucleate meronts, and sporonts, or chains of cells have not been observed in other *Nosema* species from the Acrididae.

DIAGNOSIS

N. montanae n.sp.

Host species. *Melanoplus packardii* (Orthoptera: Acrididae).

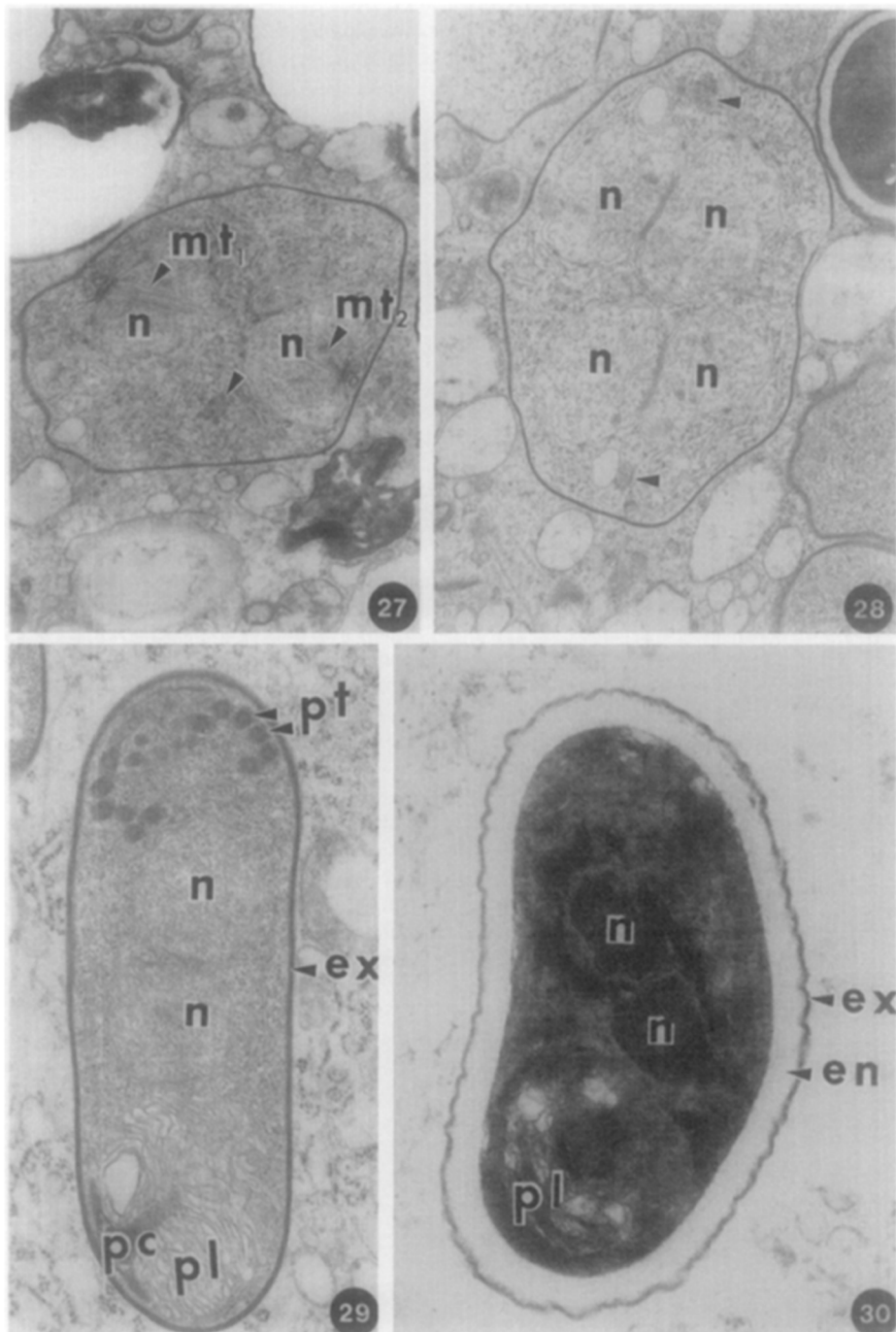


FIG. 27. A sporont undergoing closed karyokinesis showing both nonkinetochore microtubules (mt₁) and kinetochore microtubules (mt₂). The solitary arrow depicts a clump of undefined cytoplasmic vesicles apparently golgi bodies (15,470 \times).

FIG. 28. A sporont with two diplokarya. The arrows depict several clumps of undefined cytoplasmic vesicles.

FIG. 29. A binucleate sporoblast with laminar polaroplast and a developing polar tube (22,100 \times).

FIG. 30. A mature binucleate spore (34,000 \times).

Infection site. Generally confined to the fat body.

Development stages. Uni-, bi-, quadri-, and multinucleate (usually octonucleate) meronts. Chains of meronts or early sporonts apparently form directly from the multinucleate meronts. Sporonts diplokaryotic, disporous. Spores ovocylindrical, somewhat curved, 3.06 ± 0.47 by $1.47 \pm 0.16 \mu\text{m}$ in fresh preparation. Somewhat smaller in Giemsa-stained preparations. Polar tube in five to seven coils.

Type material. Holotype and two paratype (Giemsa-stained) slides deposited with U.S. National Museum, Division of Echinoderms and Lower Invertebrates. Three paratype slides in type collection at U.S. Department of Agriculture, Agricultural Research Service, Rangeland Insect Laboratory, Montana State University, Bozeman, Montana 59717.

ACKNOWLEDGMENT

The authors are grateful to E. A. Oma, Microbiologist, U.S. Department of Agriculture, Agricultural Research Service, Rangeland Insect Laboratory, for her assistance with this study.

REFERENCES

- AVERY, S. W., AND ANTHONY, D. W. 1984. Ultrastructural study of early development of *Nosema algerae* in *Anopheles albimanus*. *J. Invertebr. Pathol.*, **42**, 87-95.
- BROOKS, W. M., HAZARD, E. I., AND BECNEL, J. 1985. Two new species of *Nosema* (Microsporida: Nosematidae) from the Mexican bean beetle *Epiclachna varivestis* (Coleoptera: Coccinellidae). *J. Protozool.* **32**, 525-535.
- CANNING, E. U., AND OLSON, A. C., JR. 1980. *Nosema lepocreadii* sp. n., a parasite of *Lepocreadium manteri* (Digenea, Lepocreadiidae) from the gut of the California grunion, *Leuresthes tenuis*. *J. Parasitol.*, **66**, 154-159.
- CANNING, E. U., AND SINDEN, R. E. 1973. Ultrastructural observations on the development of *Nosema algerae* Vávra and Undeen (Microsporida, Nosematidae) in the mosquito *Anopheles stephensi* Liston. *Protistologica*, **9**, 405-415.
- GRAY, F. H., CALI, A., AND BRIGGS, J. D. 1969. Intracellular stages in the life cycle of the microsporidian *Nosema apis*. *J. Invertebr. Pathol.*, **14**, 391-394.
- HENRY, J. E. 1985. *Melanoplus* spp. In "Handbook of Insect Rearing Vol. I" (P. Singh and R. F. Moore, Eds.), pp. 451-464. Elsevier, Amsterdam.
- KELLEN, W. R., AND LINDEGREN, J. E. 1969. Host-pathogen relationships of two previously undescribed microsporidia from the Indian-meal moth, *Plodia interpunctella* (Hübner), (Lepidoptera: Phycitidae). *J. Invertebr. Pathol.*, **14**, 328-335.
- SPRAGUE, V. 1977. Classification and phylogeny of the microsporidia. In "Comparative Pathobiology Vol. 2., Systematics of the Microsporidia" (L. A. Bulla and T. E. Cheng, Eds.), pp. 1-30. Plenum, New York.
- STREETT, D. A., AND HENRY, J. E. 1987. Ultrastructural investigation of the microsporidium *Nosema cuneatum* (Microspora: Nosematidae) in the grasshopper *Melanoplus sanguinipes* (Orthoptera: Acrididae) with emphasis on mitosis. *Eur. J. Protistol.*, **23**, 18-27.
- TOQUEBAYE, B. S., AND MARCHAND, B. 1984. Etude ultrastructurale des stades de développement et de la mitose sporogonique de *Nosema henosepilachnae* n. sp. (Microsporida, Nosematidae) parasite de *Henosepilachna elaterii* (Rossi, 1794) (Coleoptera, Coccinellidae).
- YOUSEFF, N. N., AND HAMMOND, D. M. 1971. The fine structure of the developmental stages of the microsporidian *Nosema apis* Zander. *Tissue Cell*, **3**, 283-294.